Journal of Systems Engineering and Electronics
Vol. 33, No. 1, February 2022, pp.80 – 90

Performance analysis of multi-group three-tuple cross-eye jamming

CHEN Jiabei, SHI Qingzhan*, HUANG Zhaoyu, WANG Qingping, and YUAN Naichang

State Key Laboratory of Complex Electromagnetic Environmental Effects of Electronics and Information System, National University of Defense Technology, Changsha 410000, China

Abstract: Monopulse radar is widely used in military. Jamming monopulse radar has always been a research hotspot in electronic warfare (EW). Cross-eye jamming has always been considered as the most effective measures to jam with monopulse radar. In this paper, we propose a multi-group three-tuple cross-eye jamming structure where each group contains three antenna elements with a definite phase and an amplitude relationship. Then, based on the principle of monopulse angle measurement, the error angle is deduced theoretically. Simulations show that such a multi-group three-tuple cross-eye jamming structure performs better than the multi-element cross-eye jamming structure previously proposed, and the analysis of the centroid shows that the centroid of the structure proposed in this paper is more widely distributed in space.

Keywords: electronic warfare (EW), angular deception jamming, cross-eye jamming, three-tuple antenna array, near field.

DOI: 10.23919/JSEE.2022.000009

1. Introduction

Cross-eye jamming is an effective angular deception jamming technique used for countering monopulse radar. Cross-eye jamming attempts to protect a military platform against the approaching active radar seekers by transmitting two jamming signals with equal amplitudes and an 180° phase shift to induce angular error into monopulse radar. As the most effective short-range self-defense jamming against monopulse radar, the research on cross-eye jamming has become a hot research topic in electronic war.

After more than half a century of developments, cross-eye jamming theory has made great progress. The development of cross-eye jamming theory can be roughly divided into three stages: artificial glint [1], two-element retrodirective cross-eye jamming (TRCJ) [2], and multi-element retrodirective cross-eye jamming (MRCJ) [3,4]. Cross-eye jamming with artificial glint, which can be physically interpreted from interference phenomena. In 2009, Du Plessis et al. [2] of the University of South Africa studied the TRCJ from the perspective of the reverse antenna structure on the monopulse radar and derived rigorous mathematical formulas of the retrodirective cross-eye jamming [5]. Beginning in 2013, Liu et al. [6,7] proposed an MRCJ based on the linear reverse antenna array and the circular reverse antenna array to overcome the constraints of practical application of TRCJ. Liu et al. [8] proposed an orthogonal multiple elements cross-eye jamming technique based on the orthogonal four-element and linear reverse array. This scheme ensures that the jamming platform can still maintain certain jamming performance when the monopulse rada is rotated, shaken, or scanned by a monopulse radar in different directions. In addition, with the development of simulation software, many scholars use simulation software to simulate cross-eye jamming scenarios to analyze jamming performance [9,10].

For the previous cross-eye jamming structure, whether it is a two-element or a linear array structure[11,12], the problem of the scattering center on extended antenna arrays cannot be completely solved, and there are strict requirements for amplitude ratio and phase shift [13]. The MRCJ structure is relatively flexible with various parameters between different pairs of antennas, which greatly reduces the utilization and flexibility of the antenna [14]. In the structure proposed in [15], by controlling the amplitude and phase of three antenna elements at the same time, the phase between antennas is no longer required to reverse, and the radar indication angle can produce errors in any direction in space. When applied to UAV platforms, the requirements for system parameters will be greatly relaxed.

The proposed structure constructs a multi-group three-tuple cross-eye jamming with each group consisting of three antenna elements with different relative amplitudes and phase shifts. In the theory proposed in [15], the

Manuscript received October 13, 2020.
*Corresponding author.

centroid (the position indicated by the monopulse radar) can be located in anywhere of the plane. This paper will analyze the jamming structure from the sum-channel signals, difference-channel signals, and the monopulse indicating angle. Compared with the traditional linear array, this structure has a better performance and does not need a phase shift of 180° and an amplitude ratio of 1:1.

Finally, the contribution of this paper can be summarized as follows:

(i) A multi-group three-tuple cross-eye jamming structure is proposed, and the rigorous mathematical expression of monopulse error is derived.

(ii) Simulation results show that the three-tuple structure would lead to a larger angular error and the jamming performance is better because it breaks through the constraint of the line array.

(iii) The simulation results show that the position of the false target generated by the multi-group three-tuple cross-eye jamming may be distributed in any position on the plane, and the line array can only be distributed on the straight line.

(iv) The results prove that the three-tuple structure in each group can compensate the originally undesired two-element structure with the third element to achieve the best jamming performance.

The rest of this paper is organized as follows: Section 2 describes the processes to derive the mathematical expressions of the monopulse indication angle and the location of the false target. Section 3 performs simulation experiments to discuss the jamming performance of the multi-group three-tuple cross-eye jamming system with the monopluse indicated angle and the location of the false target. Finally, a brief conclusion is give in Section 4.

2. Mathematical analysis

2.1 Jamming scenario

We consider the jamming scenario of a multi-group three-tuple system against phase-comparison monopulse radar. The jamming system consists of multiple groups, each of which consists of three antenna elements with a definite phase and an amplitude relationship. As shown in Fig.1, the three elements of each group are located in three positions (top, bottom, middle) of the target center. From the outside group to the inside, we number each group as 1, 2, 3, ⋯. Similar to the MRCJ, the signal received by one jamming antenna element would be transmitted to another through a certain amplitude gain and a certain phase shift. The difference is that in each group, the signal received by the middle antenna element (antenna element located in front of the target center) will be sent by the top antenna element (antenna element located above the target center), while the signal received by the top jamming element will be sent by the bottom jamming element (antenna element located below the target center). The signal received by the bottom element will be sent by the middle jamming element. We assume that the range from the radar to the center of the jammer is r, the spacing of the phase centers of the phase-comparison monopulse antenna elements is d_p, the angle to the center of the jammer measured from the radar boresight is θ_r, and the rotation of the jammer is θ_c. The overall base length of the jammer antenna array from the top antenna of the outermost group to the bottom antenna of the outermost group is d_c. Fig. 2 shows the signal receiving and sending process of each group. This constitutes a jamming group of three jamming antenna elements. Theoretically, such a group can be expanded from one group to a infinite number of groups. Next, we will analyze the performance of this scenario.

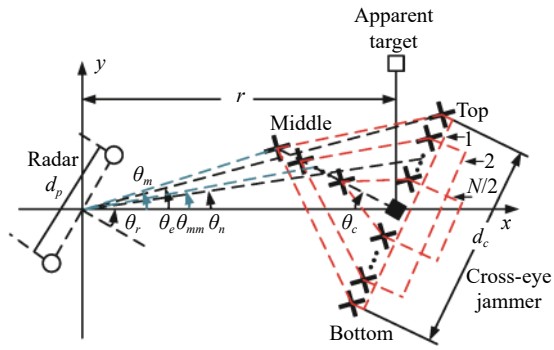

Fig. 1 Geometry of a multi-group three-tuple cross-eye jamming scenario

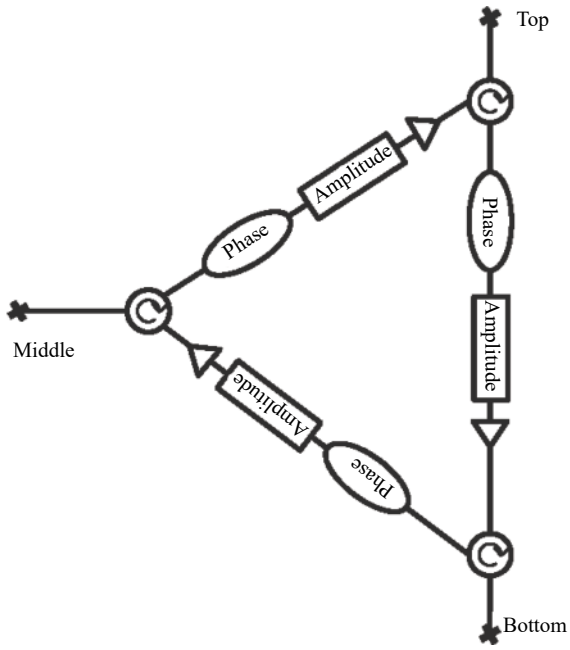

Fig. 2 Process of signal reception and transmission in each group

The jammer antenna elements from the top antenna to the bottom antenna have a uniform spacing d_a, which can be calculated by

$$d_a = \frac{d_c}{N-1}. \tag{1}$$

Different three-tuple structures only affect the difference of phase and the phase shifts caused by structures can be accurately compensated by calculating the differences of three propagation paths. For simplicity, assume the length of the jammer antenna array from the target center to the middle antenna of the outermost group is d_m, where

$$d_m = \frac{d_c}{2}. \tag{2}$$

In addition, there is a uniform spacing between the middle antenna elements as d_a.

The array from the top antenna to the bottom antenna of the outermost group has a half-angle of θ_e for the radar boresight, given by geometric relationship

$$\tan(\theta_e) = \frac{d_c \cos\theta_c/2}{r \pm d_c \sin\theta_c/2}. \tag{3}$$

In a real scene, the cross-eye jammer should be in the far field of the monopulse radar, meaning $r \gg d_c$, therefore

$$\theta_e \approx \frac{d_c \cos\theta_c}{2r}. \tag{4}$$

The half angle θ_n of the jamming loop n for the radar boresight is

$$\theta_n = F_n \theta_e \tag{5}$$

in which

$$F_n = \frac{N+1-2n}{N-1}. \tag{6}$$

Define F_n as the group baseline ratio, which represents the ratio of the jamming group n baseline to the total baseline length of the antenna array. The array from the middle antenna of the outmost group to the target center has an angle of θ_m for the radar boresight with

$$\tan\theta_m = \frac{d_m \sin\theta_c}{r - d_m \cos\theta_c}, \tag{7}$$

$$\theta_m \approx \frac{d_m \sin\theta_c}{r}, \tag{8}$$

and the radar boresight for loop n is

$$\theta_{mn} = F_n \theta_m. \tag{9}$$

2.2 Mathematical derivation of the monopulse error

Based on previous research conclusions [3], the model proposed in this paper can obtain that the sum-channel normalized signals of the top element S_{tn}, the bottom element S_{bn} and the middle element S_{mn} from jammer group n ($n = 1, 2, \cdots$) are

$$\begin{cases} S_{tn} = \cos(k_{sn} + k_{cn}) P_r(\theta_r + \theta_e) \\ S_{bn} = \cos(k_{sn} - k_{cn}) P_r(\theta_r - \theta_e) \\ S_{mn} = \cos(k_{smn} + k_{cmn}) P_r(\theta_r + \theta_{mn}) \end{cases}. \tag{10}$$

The difference-channel normalized signals of the top element D_{tn}, the bottom element D_{bn} and the middle element D_{mn} from the jammer group n are

$$\begin{cases} D_{tn} = \mathrm{j}\sin(k_{sn} + k_{cn}) P_r(\theta_r + \theta_e) \\ D_{bn} = \mathrm{j}\sin(k_{sn} - k_{cn}) P_r(\theta_r - \theta_e) \\ D_{mn} = \mathrm{j}\sin(k_{smn} + k_{cmn}) P_r(\theta_r + \theta_{mn}) \end{cases} \tag{11}$$

where

$$\begin{cases} k_{sn} = \beta \dfrac{d_p}{2} \sin\theta_r \cos\theta_n \\ k_{cn} = \beta \dfrac{d_p}{2} \cos\theta_r \sin\theta_n \\ k_{smn} = \beta \dfrac{d_p}{2} \sin\theta_r \cos\theta_{mn} \\ k_{cmn} = \beta \dfrac{d_p}{2} \cos\theta_r \sin\theta_{mn} \end{cases}. \tag{12}$$

In jammer group n, we assume that the signal passing from the middle antenna element to the top element has an amplitude gain of a_{mtn} and phase shift of φ_{mtn}. The signal passing from the top antenna element to the bottom element has an amplitude gain of a_{tbn} and phase shift of φ_{tbn}. The signal passing from the bottom antenna element to the middle element has an amplitude gain of a_{bmn} and phase shift of φ_{bmn}. According to the jamming process we described earlier, the sum-channel signals S_{Jn} and difference-channel signals D_{Jn} received by monopluse radar from jammer group n are given by

$$\begin{aligned} S_{Jn} = {} & A_{mtn} S_{mn} P_c(\theta_c + \theta_{mn}) S_{tn} P_c(\theta_c + \theta_n) + \\ & A_{tbn} S_{tn} P_c(\theta_c + \theta_n) S_{bn} P_c(\theta_c - \theta_n) + \\ & A_{bmn} S_{bn} P_c(\theta_c - \theta_n) S_{mn} P_c(\theta_c + \theta_{mn}), \end{aligned} \tag{13}$$

$$\begin{aligned} D_{Jn} = {} & A_{mtn} S_{mn} P_c(\theta_c + \theta_{mn}) D_{tn} P_c(\theta_c + \theta_n) + \\ & A_{tbn} S_{tn} P_c(\theta_c + \theta_n) D_{bn} P_c(\theta_c - \theta_n) + \\ & A_{bmn} S_{bn} P_c(\theta_c - \theta_n) D_{mn} P_c(\theta_c + \theta_{mn}), \end{aligned} \tag{14}$$

where

$$\begin{cases} A_{mtn} = a_{mtn} \mathrm{e}^{\mathrm{j}\varphi_{mtn}} \\ A_{tbn} = a_{tbn} \mathrm{e}^{\mathrm{j}\varphi_{tbn}} \\ A_{bmn} = a_{bmn} \mathrm{e}^{\mathrm{j}\varphi_{bmn}} \end{cases}. \tag{15}$$

$P_r(\theta_r + \theta_n)$ is the gain of the radar antenna on $\theta_r + \theta_n$, $P_c(\theta_c + \theta_n)$ is the gain of the jamming antenna on

$\theta_c+\theta_n$. Since θ_n and θ_{mn} are small, we can make the following approximation:

$$\begin{cases} P_r(\theta_r\pm\theta_n)\approx P_r(\theta_r+\theta_{mn})\approx P_r(\theta_r) \\ P_c(\theta_c\pm\theta_n)\approx P_c(\theta_c+\theta_{mn})\approx P_c(\theta_c) \end{cases}. \tag{16}$$

In addition, define

$$P_n = P^2{}_r(\theta_r)P^2{}_c(\theta_c). \tag{17}$$

Substitute (10), (11) into (13), (14):

$$\begin{aligned} S_{Jn} = P_n[&A_{mtn}\cos(k_{smn}+k_{cmn})\cos(k_{sn}+k_{cn})+ \\ &A_{tbn}\cos(k_{sn}+k_{cn})\cos(k_{sn}-k_{cn})+ \\ &A_{bmn}\cos(k_{sn}-k_{cn})\cos(k_{smn}+k_{cmn})] = \\ &\frac{1}{2}P_n[A_{mtn}(\cos\chi_{1n}+\cos\chi_{2n})+ \\ &A_{tbn}\cos(2k_{sn}+\cos 2k_{cn})+ \\ &A_{bmn}\cos(\chi_{3n}+\cos\chi_{4n})] \end{aligned} \tag{18}$$

$$\begin{aligned} D_{Jn} = \mathrm{j}P_n[&A_{mtn}\cos(k_{smn}+k_{cmn})\sin(k_{sn}+k_{cn})+ \\ &A_{tbn}\cos(k_{sn}+k_{cn})\sin(k_{sn}-k_{cn})+ \\ &A_{bmn}\cos(k_{sn}-k_{cn})\sin(k_{smn}+k_{cmn})] = \\ &\mathrm{j}\frac{1}{2}P_n[A_{mtn}(\sin\chi_{1n}-\sin\chi_{2n})+ \\ &A_{tbn}(\sin 2k_{sn}-\sin 2k_{cn})+ \\ &A_{bmn}(\sin\chi_{3n}-\sin\chi_{4n})] \end{aligned} \tag{19}$$

where

$$\begin{cases} \chi_{1n} = k_{smn}+k_{cmn}+k_{sn}+k_{cn} \\ \chi_{2n} = k_{smn}+k_{cmn}-k_{sn}-k_{cn} \\ \chi_{3n} = k_{sn}-k_{cn}+k_{smn}+k_{cmn} \\ \chi_{4n} = k_{sn}-k_{cn}-k_{smn}-k_{cmn} \end{cases}. \tag{20}$$

When $N/2$ groups work together

$$\begin{aligned} S_J = \frac{1}{2}\sum_{n=1}^{\frac{N}{2}} P_nC_n[&A_{mtn}(\cos\chi_{1n}-\cos\chi_{2n})+ \\ &A_{tbn}(cos2k_{sn}-\cos 2k_{cn})+ \\ &A_{bmn}(\cos\chi_{3n}-\cos\chi_{4n})] \end{aligned} \tag{21}$$

and

$$\begin{aligned} D_J = j\frac{1}{2}\sum_{n=1}^{\frac{N}{2}} P_nC_n[&A_{mtn}(\sin\chi_{1n}-\sin\chi_{2n})+ \\ &A_{tbn}(\sin 2k_{sn}-\sin 2k_{cn})+ \\ &A_{bmn}(\sin\chi_{3n}-\sin\chi_{4n})]. \end{aligned} \tag{22}$$

C_n indicates the difference between the groups where $C_n = c_n\mathrm{e}^{\mathrm{j}\phi_n}$. When $A_{mtn}=1$, $A_{bmn}=0$, $k_{smn}=k_{sn}$, $k_{cmn}=k_{cn}$, which means $\theta_n=\theta_{mn}$ and the bottom → middle loop does not work, the sum-channel and difference-channel functions are the same as the TRCJ. Consistently, it is shown that the TRCJ is a special case of the multi-group three-tuple jamming proposed in this paper. Besides, the multi-group three-tuple jamming expands the degree of freedom of the traditional cross-eye jamming.

The accurate monopulse processor normalizes the difference-channel signal with the sum-channel signal, and the monopulse error will be

$$M_J = \Im\left(\frac{D_J}{S_J}\right). \tag{23}$$

$\Im$ is the sign of the imaginary part of the complex number. The monopulse indicated angle θ_i could be converted from the monopulse error in (23) by using the relationship as follows:

$$\tan\left[\frac{\beta d_p}{2}\sin\theta_i\right] = M_J. \tag{24}$$

Next, we simplify (24) to get a more concise monopulse error. Triangle approximation in [11] has shown

$$\cos 2k_{c1} = \cos[\beta d_p\cos\theta_r\sin\theta_e]\approx 1. \tag{25}$$

This approximation means that when $\theta_e \ll \beta d_p$, $2k_{c1}$ approaches to zero.

Furthermore, we can get

$$\begin{cases} \cos k_{cn}\approx\cos k_{cmn}\approx 1 \\ k_{cn}\approx F_nk_{c1} \\ k_{cmn}\approx F_nk_{cm1} \\ \sin k_{cn}\approx F_n\sin k_{c1} \\ \sin k_{cmn}\approx F_n\sin k_{cm1} \\ k_{smn}\approx k_{sn}\approx\beta d_p\sin\theta_r \end{cases}. \tag{26}$$

Then, we could change (24) into

$$M_J = \Im\left(\frac{D_J}{S_J}\right)\approx \Re\left(\frac{\sum_{n=1}^{\frac{N}{2}}[\Gamma_{mtn}+\Gamma_{tbn}+\Gamma_{bmn}]}{\sum_{n=1}^{\frac{N}{2}}[(A_{mtn}+A_{tbn})(\cos 2k_{s1}+1)-A_{bmn}]}\right), \tag{27}$$

where $\Re$ is the sign of the real part of the complex number, and

$$\begin{cases} \Gamma_{mtn} = A_{mtn}\sin(2k_{s1} + F_n(k_{c1} + k_{cm1})) \\ \Gamma_{tbn} = A_{tbn}(\sin 2k_{s1} - F_n \sin 2k_{c1}) \\ \Gamma_{bmn} = A_{bmn}(\sin 2k_{s1} - F_n \sin(k_{c1} + k_{cm1})) \end{cases}. \tag{28}$$

Different from the jamming of the TRCJ, the center of the multi-group three-tuple cross-eye jamming is located in the line array or its extension line. The monopulse indicated angle of the multi-group three-tuple jamming will be based on the jamming amplitude gain and the phase shift of the three directions, by setting different parameters, the center point of the jammer can theoretically be anywhere in the space [15]. Therefore, we do not derive the cross-eye gain. In addition, in the following experiments, we will compare the change of the monopulse indicated angle with non jammed and jammed cases, to show the performance of the proposed jamming method.

Because of the complexity of the multi-group, we only derive the target center location of one-group cases. In the previous section, we mentioned that the target center of the three antenna elements would be on the plane of the three antenna elements. We reestablished the coordinate system as shown in Fig. 3, because it is generally believed that the transmission time of the signal determines the distance of the false target to the radar, while the sum-difference signal determines the position. In other words, the distance between the false target and the radar should be the same as the distance of the real target between the radar, and the specific location should be at other locations with the same distance. To reduce the effect of phase difference caused by propagation, we reposition the positions of the three antenna elements. In Fig. 3, we consider that the plane of the three antenna elements is parallel to the plane of the monopulse radar, and O' is the center of monopluse radar. Of course, this attitude of the aircraft can also be considered as the projection of other flight attitudes on this plane. Derivation in [16] shows the components of the electromagnetic field in the x, y, and z directions as

$$\begin{cases} X = \dfrac{1}{\eta}(a_{mtn}^2 + a_{tbn}^2 + a_{bmn}^2 + 2a_{mtn}a_{tbn}\cos\varphi_{tbn} + \\ \quad 2a_{tbn}a_{bmn}\cos\varphi_{bmn} + 2a_{mtn}a_{bmn}\cos\varphi_{mtn}) \\ Y = \dfrac{1}{\eta}(a_{tbn}^2 + a_{mtn}a_{tbn}\cos\varphi_{tbn} + \dfrac{3}{2}a_{tbn}a_{bmn}\cos\varphi_{bmn} + \\ \quad \dfrac{1}{2}a_{bmn}^2 + \dfrac{1}{2}a_{mtn}a_{bmn}\cos\varphi_{mtn}) \\ Z = \dfrac{1}{\eta}\Theta_{\max}[(a_{bmn}^2 + a_{mtn}a_{bmn}\cos\varphi_{mtn} + a_{tbn}a_{bmn}\cos\varphi_{bmn}) + \\ \quad \dfrac{1}{2}\Phi_{\max}(a_{tbn}a_{bmn}\cos\varphi_{bmn} + \dfrac{1}{2}a_{bmn}^2)] \end{cases} \tag{29}$$

where η is the parameter of the electromagnetic field. $\Theta_{\max}$ is the maximum elevation angle of the three elements, $\Phi_{\max}$ is the maximum azimuth of the three elements.

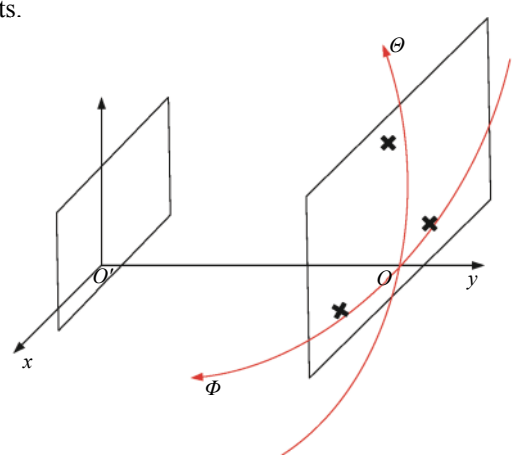

Fig. 3 Azimuth and pitch angle of a three-antenna elements simulation target

We can get the azimuth angle of the scattering points as

$$\Phi = \arctan\left(\frac{Z}{\sqrt{X^2 + Y^2}}\right) \tag{30}$$

and the pitch angle as

$$\Theta = \arctan\left(\frac{Y}{X}\right). \tag{31}$$

According to (31) and (32), if there are only two elements, then $a_{mtn} = a_{bmn} = 0$, the Z component in the equation will be 0, that is to say, the scattering center can only be deviated from the true scattering center in the pitch angle, and there will be no jamming effect on the azimuth angle. This is one of the reasons why the three-element case is better than the two-element case.

3. Simulation results

The degrees of freedom of a multi-group three-tuple cross-eye jammer are too large to analyze. Without loss of generality, one-group and two-group cross-eye jammer is employed as the typical implementation of a multi-group three-tuple jamming system in this section. The typical parameters of a missile threatening an aircraft or ship are given as follows:

(i) Radar carrier frequency: 9 GHz;

(ii) Radar beam width: $10°$;

(iii) Radar antenna apertures: 2.54λ;

(iv) Jammer range: 1 km;

(v) Array base length: 10 m;

(vi) Jammer rotation: $30°$.

In order to compare the jamming performance of two-element and multi-group three-tuple cross-eye jamming,

we set $a_{bmn} = 1$ and $\varphi_{bmn} = 0$.

First, we analyze sum-channel and difference-channel signals under two-element jamming and one-group three-tuple jamming. As shown in Fig. 4 and Fig. 5, within a beam, the sum-channel and difference-channel signals of two-element and one-group three-tuple cross-eye jamming are almost the same. Under the monopulse angle measurement, the difference-channel signal is used to generate the radar indication angle. As Fig. 4 shows, the difference in the signal of the difference-channel is due to the change in the indicated angle caused by adding a third jamming element. The sum-channel mainly normalized the difference-channel signal in the monopulse angle measurement. Fig. 5 shows that the sum-channel under three-tuple jamming is less than the two-element jamming. This is because when the system parameters are close to ideal, the frontal signal of the jamming group will cancel at the radar antenna, which reduces the amplitude of the channel signal. Although the channel signal has symbol change and beam jitter near the zero of the first beam, it is important that the error angle is basically linear within the 3 dB beam width, whether the radar beam width is 10° or 20°.

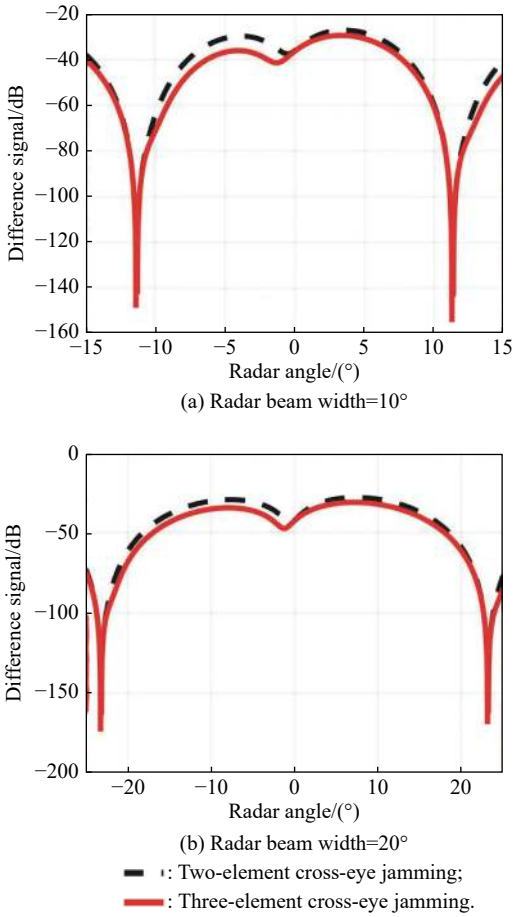

Fig. 4 Value of difference-channel signal

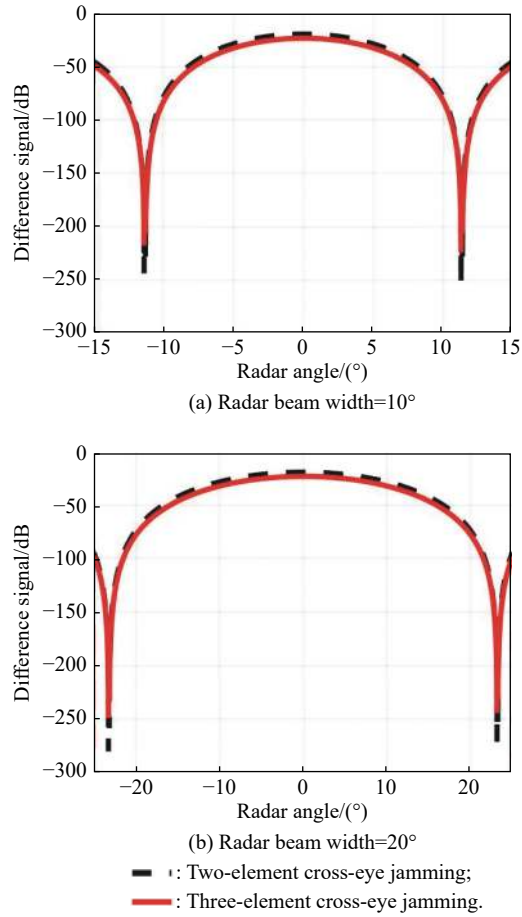

Fig. 5 Value of sum-channel signal

The monopulse indicated angle can directly show the effect of jamming. Fig. 6 shows the monopulse indicated angle curve in the one-group case. The blue dotted curve shows the two-element jamming case and the black dotted curve shows the no jamming case. Obviously, in the case of no jamming, the angle of the radar and the indicated angle should be equal, that is to say, it should be a positive proportion curve in Fig. 6. At the same time, when the indicated angle curve is farther away from the curve of no jamming with 3 dB beam width, the larger the angle error is, the better the jamming effect is. Different curves represent the relationship between the indicated angle and the error angle under different φ_{mt1} and a_{mt1}. It can be seen that after adding the third element and choosing proper parameters of the third element, the monopulse indicated angle error becomes larger, making a monopulse deviate from the true direction of the target more than the two-element cases. The group jamming system with poor jamming performance can be well compensated by choosing an appropriate third parameter and cause a greater angle error or even break a monopulse radar lock (this requires very accurate parameters in the two-element cross-eye case). Of course, not all three-tuple cross-eye jamming produces an error angle greater

than the two-element cross-eye jamming, because if the inappropriate array element parameters have been selected, the sum-channel signal of the monopulse radar would increase, thereby making the indicated error angle smaller.

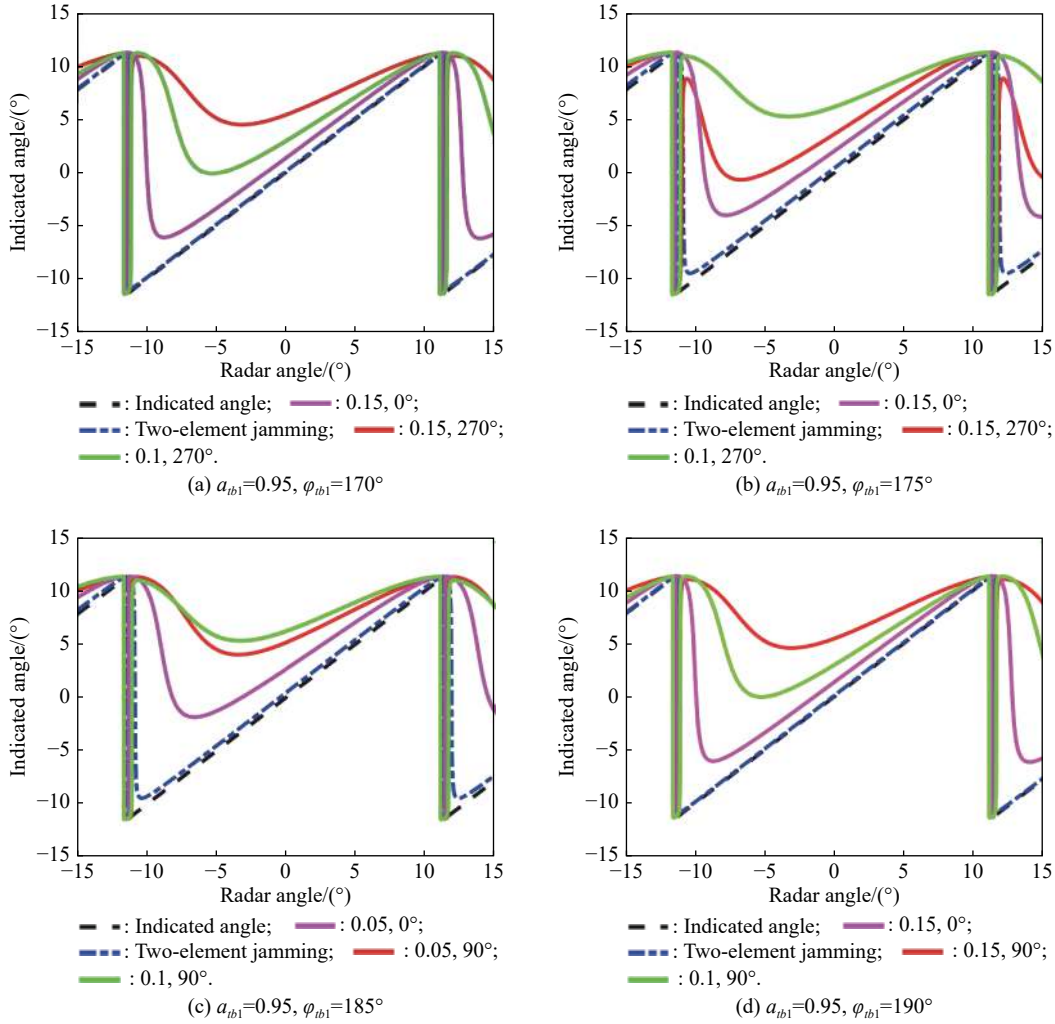

Fig. 6 Indicated angle curves for different values with one group

Fig. 7 shows the cases of two-group jamming, while different curves represent the relationship between the indicated angle and the error angle under different a_{mt1}, φ_{mt1} and a_{mt2}, φ_{mt2}. In Fig. 7(a) and Fig. 7(d), similar to the one-group cases, the third element is added, which gives the radar indication angle a larger error, and even breaks a monopulse radar lock, and in Fig. 7(b), it can be seen that adding the third element has not greatly affected the jamming performance. This is because the other two elements in Fig. 7(b) have already had compensation, and the third element would be unimportant in the ideal parameter scene. Fig. 7(c) shows that even in the two-group-case, inappropriate element parameters still have a bad effect on the jamming performance. In cross-eye jamming, the most significant effect on the jamming performance is the phase shift and amplitude gain of each element. Next, we would analyze the effect of phase shift on the monopulse radar indicated angle. Fig. 8 shows the indicated angle with different φ_{tb1} conditions in a one-group case where a_{tb1} = 0.95. First, even if a third element is not added, only two elements can cause an error angle. After the third element is added, the indication angle changes significantly, and according to the original parameter configuration, the phase shift of the third element is not the same when the maximum indication angle is obtained. What can be seen is that when the phase shift between the two-element cross-eye jamming is less than 180°, the optimal value of the third element is more than 180°. On the contrary, the optimal value would be less than 180°. Besides, as shown in Fig. 8(a) and Fig. 8(b), even if there is a third element as compensation for the two-element scene, the jamming effect can only be improved to a certain extent.

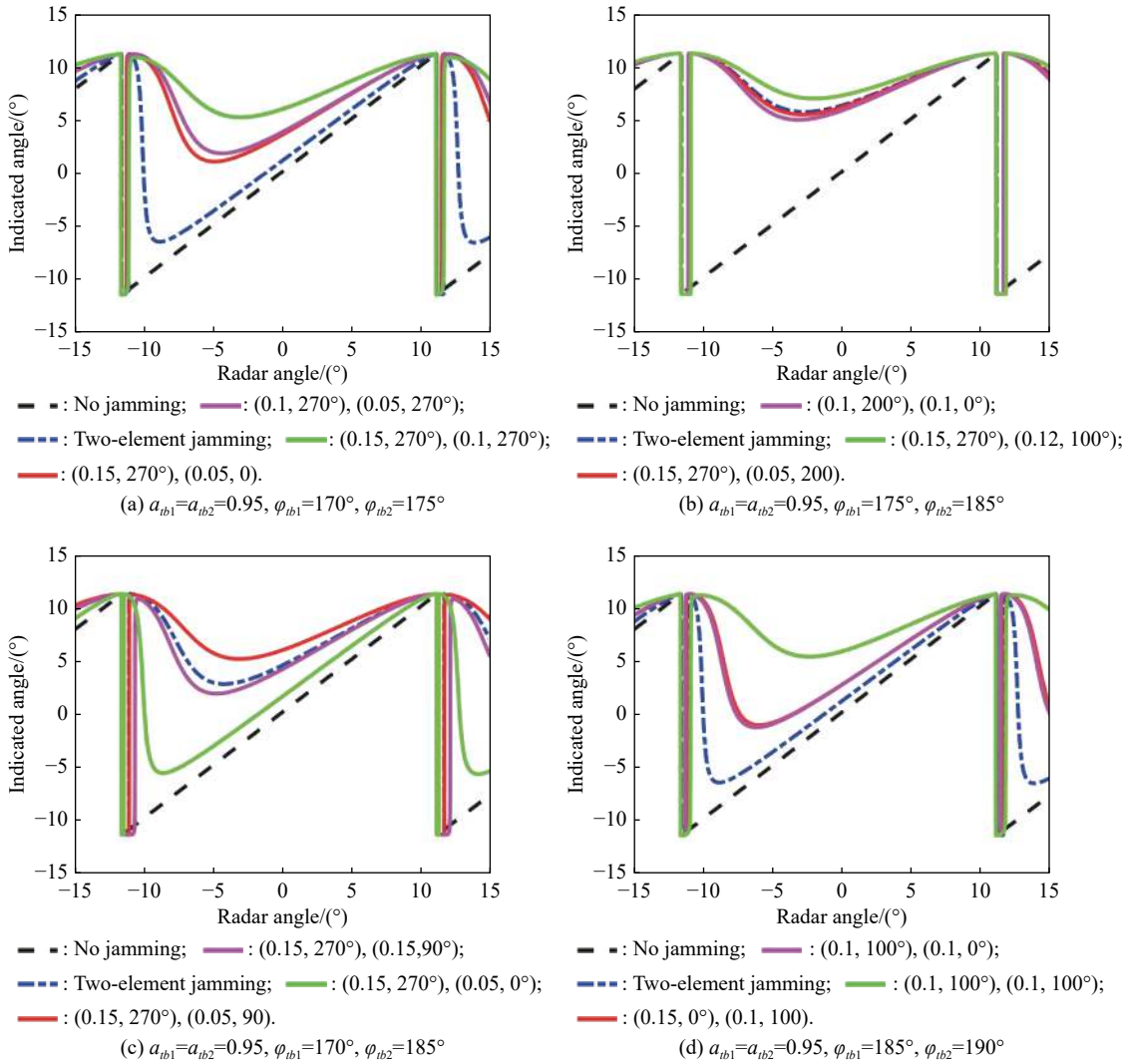

Fig. 7 Indicated angle curves for different values with two groups

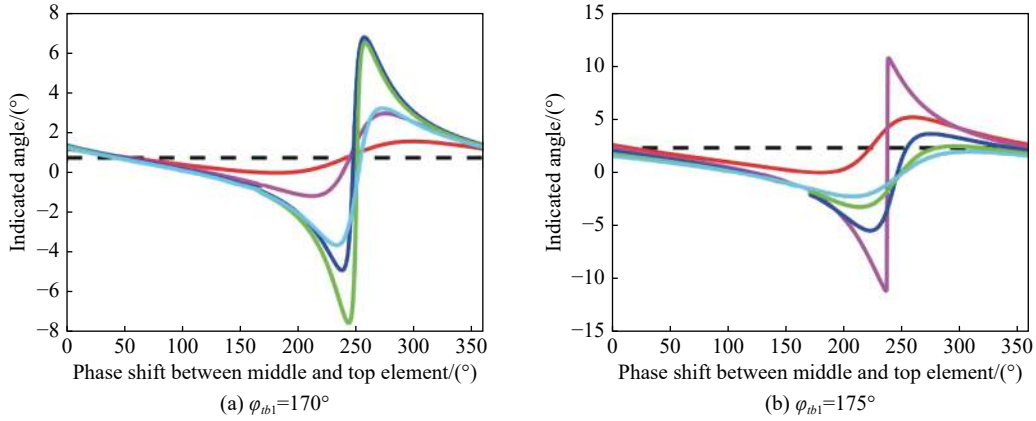

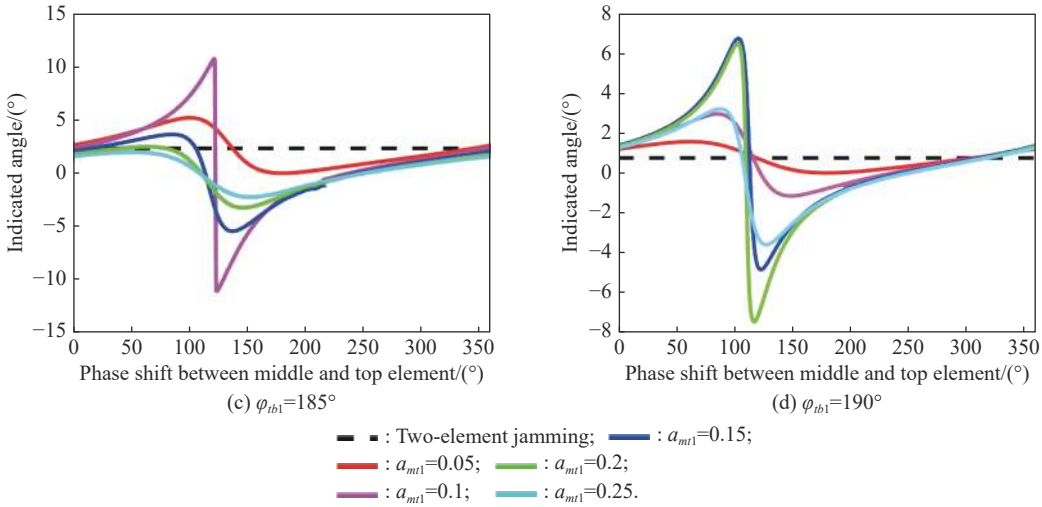

Fig. 8 Indicated angle curves for different phase shifts

As shown in Fig. 9, a proper φ_{mt1} can improve the jamming performance in a large extent, and most of the optimal a_{mt1} is concentrated between 0 and 0.2. This is because the main purpose of adding a third element is to compensate the undesired two-element jamming structure. Therefore, the amplitude does not need to be too large. If it is too large, the sum-channel signal of the monopulse radar would increase, making the target a beacon. In addition, the proper value of φ_{mt1} and proper value of a_{mt1} can be used to increase the error angle to a maximum extent, and the error angle reaches 6.53°.

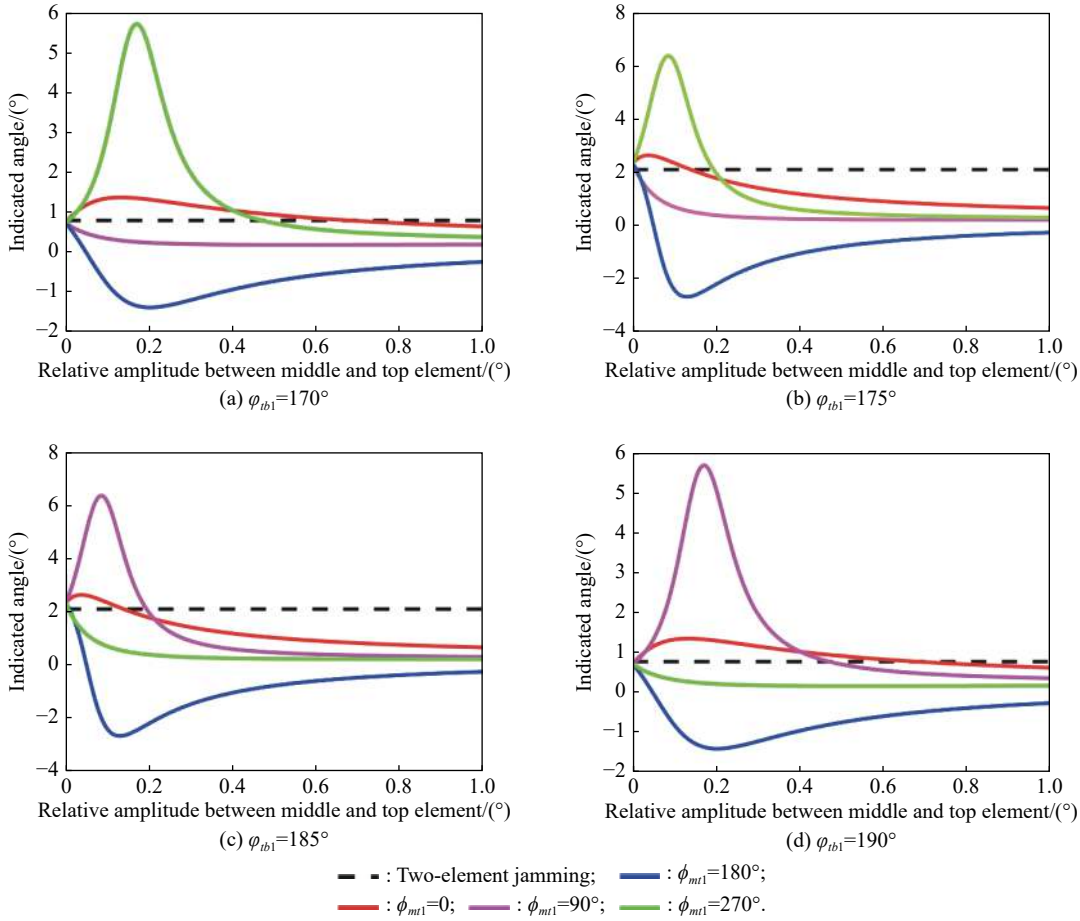

Fig. 9 Indicated angle curves for different relative amplitudes

By observing Fig. 8 and Fig. 9, when an error angle is determined, we can determine the approximate range of phase shift and amplitude gain requirements. In practical application, with the improvement of the accuracy of the current equipment, the value in this range can be achieved.

The advantage of the three-tuple cross-eye jamming comparing the two-element cross-eye is not only that the generated angular error is greater, but also because the three-tuple jamming can generate false targets at any position in the area where it is located. Fig. 10(c) is a scatter plot of the near field radiation center of the two-element jamming. The red * in the figure indicates the position of the array element. Most of the radiation centers are concentrated near the two array elements. The radiation scattering points decrease when the distance increases. In Fig. 10(d), by adding a third element, the position of the scattering points is distributed in three directions, unlike a two-element jamming with only two directions on the extension of two elements. In Fig. 10(c) and Fig. 10(d), the farther away the scattering points are, the more sparse they are. It can also be found in Fig. 8 and Fig. 9, that the area with a larger indicator angle has a larger gradient, and the area with a smaller indicator angle has a smaller gradient, which indicates that the cross-eye jamming angular error does not change linearly with the amplitude gain or the phase shift, but changes exponentially with the amplitude gain or the phase shift.

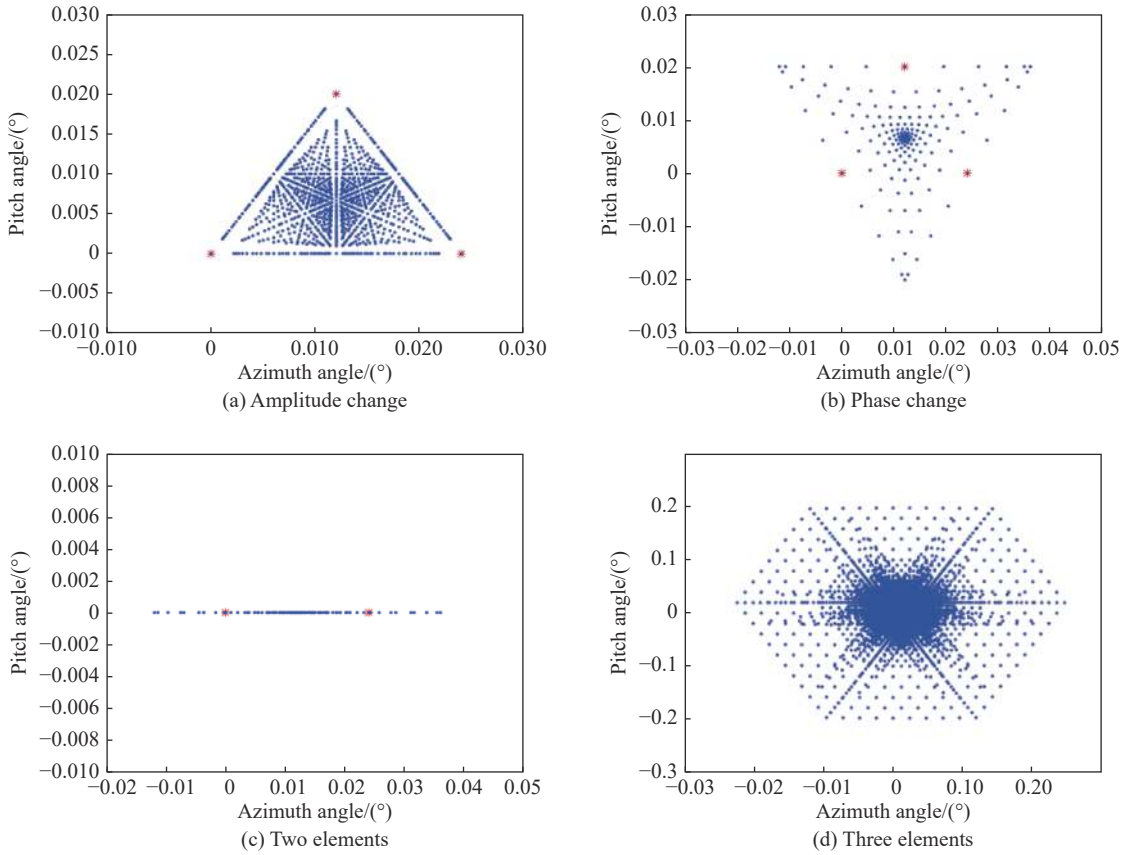

Fig. 10 Position of scatter points

Fig. 10(a) shows that when the phase difference between the three-tuple is 0, no matter how the relative amplitude ratio between the three-tuple changs, the point of the false target generated is always within the three-tuple. And when the amplitude ratio between the three-tuple is 1 and the phase shift changes from 0 to π, as shown in Fig. 10(b), a part of the false target positions are also within the array elements, and a large part of the false targets are outside the three-tuple. From the perspective of the monopulse angle measurement system, an angular error has been generated.

4. Conclusions

A basic and rigorous mathematical analysis of multi-group three-tuple cross-eye jamming employing a triad linear array is proposed in this paper. The main contribution is that the mathematical derivations of the monopulse error and the location of the near field radiation center are presented. Furthermore, simulation results demonstrate that the model proposed in this paper has a better performance in comparison with the TRCJ in induced angular error and location of radiation center. Importantly, in

practical scenarios, due to the factors such as device and weather, the phase shift and amplitude gain cannot reach the ideal value, the system proposed in this paper improves jamming performance by adding an element, but the amplitude gain of the newly added element should not be too large. If the amplitude gain is too large, the echo of the whole system will become stronger and become a beacon. Generally speaking, it can be between 0 and 0.2. The phase shift of the new element is about π, and the phase shift greater or less than π is mainly opposite to the phase shift of the original system.

References

[1] SHIZUME P K. Angular deception countermeasure system. US: United States Patent 4117484, 1978.

[2] DU PLESSIS W P. A comprehensive investigation of retrodirective cross-eye jamming. Pretoria: University of Pretoria, 2010.

[3] LIU T P, LIAO D P, WEI X Z, et al. Performance analysis of multiple-element retrodirective cross-eye jamming based on linear array. IEEE Trans. on Aerospace and Electronics Systems, 2015, 51(3): 1867–1876.

[4] LIU T P, WEI X Z, PENG B, et al. Tolerance analysis of multiple-element linear retrodirective cross-eye jamming. Journal of Systems Engineering and Electronics, 2020, 31(3): 460–469.

[5] ODENDALL J, JOUBERT J. Tolerance analysis of cross-eye jamming systems. IEEE Trans. on Aerospace and Electronic Systems, 2011, 47(1): 740–745.

[6] LIU T P, WEI X Z, LI L. Multiple-element retrodirective cross-eye jamming against amplitude-comparison monopulse radar. Proc. of the 12th International Conference on Signal Processing, 2014: 2135–2140.

[7] LU J R, LIU T P, LIU Z, et al. Analysis of multi-loop retrodirective cross-eye jamming system for large platform. Proc. of the Progress In Electromagnetics Research Symposium, 2017: 565–572.

[8] LIU S Y, DONG C X, XU J, et al. Analysis of rotating cross-eye jamming. IEEE Antennas and Wireless Propagation Letters, 2015, 14: 939–942.

[9] KALINBSCAK I, PEHLIVAN M, YEGIN K. Cross-eye monopulse jammer located on UAV. Proc. of the Progress in Electromagnetics Research Symposium, 2017: 2032–2035.

[10] JO J, AHN J. A study on jamming technique against monopulse type missile. Proc. of the International Conference on Information and Communication Technology Convergence, 2017: 996–998.

[11] LIU W, MENG J, ZHOU L. Research on rectangular array retrodirective cross-eye jamming method considering target echo. Proc. of the 19th IEEE International Conference on Communication Technology, 2019: 224–227.

[12] LIU W, MENG J, ZHOU L. Method of four-element retrodirective cross-eye jamming based on DoA. IEEE Access, 2020, 8: 76896–76902.

[13] SONG Z Y, LI G Q, FU Q. Principle analysis of coherent two-point source jamming based on amplitude comparison monopulse. Proc. of the 3rd International Conference on Electronic Information Technology and Computer Engineering, 2019: 919–923.

[14] CHENG Y, LIU T, HUO K, et al. Analysis of performance of shipborne cross-eye jamming against anti-ship missile Proc. of the Photonics & Electromagnetics Research Symposium, 2019: 2763-2769.

[15] YU Z. Modeling and spatial electromagnetic field analysis of multivariate vector radiation source based on UAV platform. Chengdu, China: University of Electronic Science and Technology of China, 2019. (in Chinese)

[16] LIU D K. Near field error correction of multiple vector synthesis. Chengdu, China: University of Electronic Science and Technology of China, 2014. (in Chinese)

Biographies

CHEN Jiabei was born in 1994. He received his M.S. degree from Hunan University in 2018. He is currently pursuing his Ph.D. degree with the College of Electronic Science and Engineering, National University of Defense Technology. His research interests include radar signal processing and electronic countermeasures.
E-mail: doublechendouble@163.com

SHI Qingzhan was born in 1990. He received his B.S. degree from Xidian University in 2013, his M.S. and Ph.D. degrees from National University of Defense Technology (NUDT), Changsha, in 2015 and 2019 respectively. He is currently a lecturer with NUDT. His research interests include radar signal processing and electronic countermeasures.
E-mail: qingzhanshi@foxmail.com

HUANG Zhaoyu was born in 1992. He received his M.S. degree in electronics and communication engineering from University of Electronic Science and Technology of China in 2018, where he is currently pursuing his Ph.D. degree with the College of Electronic Science and Engineering, National University of Defense Technology, Changsha, China. His current research interests include passive radio frequency/microwave circuits, microstrip antennas, and wireless communication.
E-mail: huangzhaoyu10@163.com

WANG Qingping rceived his Ph.D. degree from the National University of Defense Technology (NUDT) of China in 2015. He is currently a lecturer with the Department of Electrical Science and Engineering, NUDT. His current research interests include high-resolution radar signal processing and anti-jamming technology.
E-mail: andywpq007@163.com

YUAN Naichang received his Ph.D. degree from University of Electronic Science and Technology in 1994. From that on, he stayed in National University of Defense Technology (NUDT) for ten years, where he became a senior researcher and group leader. He is currently a full professor with the Department of Electrical Science and Engineering, NUDT. His current research interests include antenna technology, electromagnetic analysis, high-resolution radar signal processing, and anti-jamming technology.
E-mail: yuannaichang@hotmail.com